Electronic Supplementary Material (ESI) for Polymer Chemistry.

Supporting Information

3D-printing of dynamic self-healing cryogels with tuneable properties

Milena Nadgorny,[1] Joe Collins,[1] Zeyun Xiao,[1] Peter. J. Scales[1] and Luke A. Connal*[2]

[1]Department of Chemical and Biomolecular Engineering, The University of Melbourne, Parkville 3010, VIC, Australia

[2]Research School of Chemistry, Australian National University, Canberra, Australian Capital Territory 2601, Australia

*Email: luke.connal@anu.edu.au

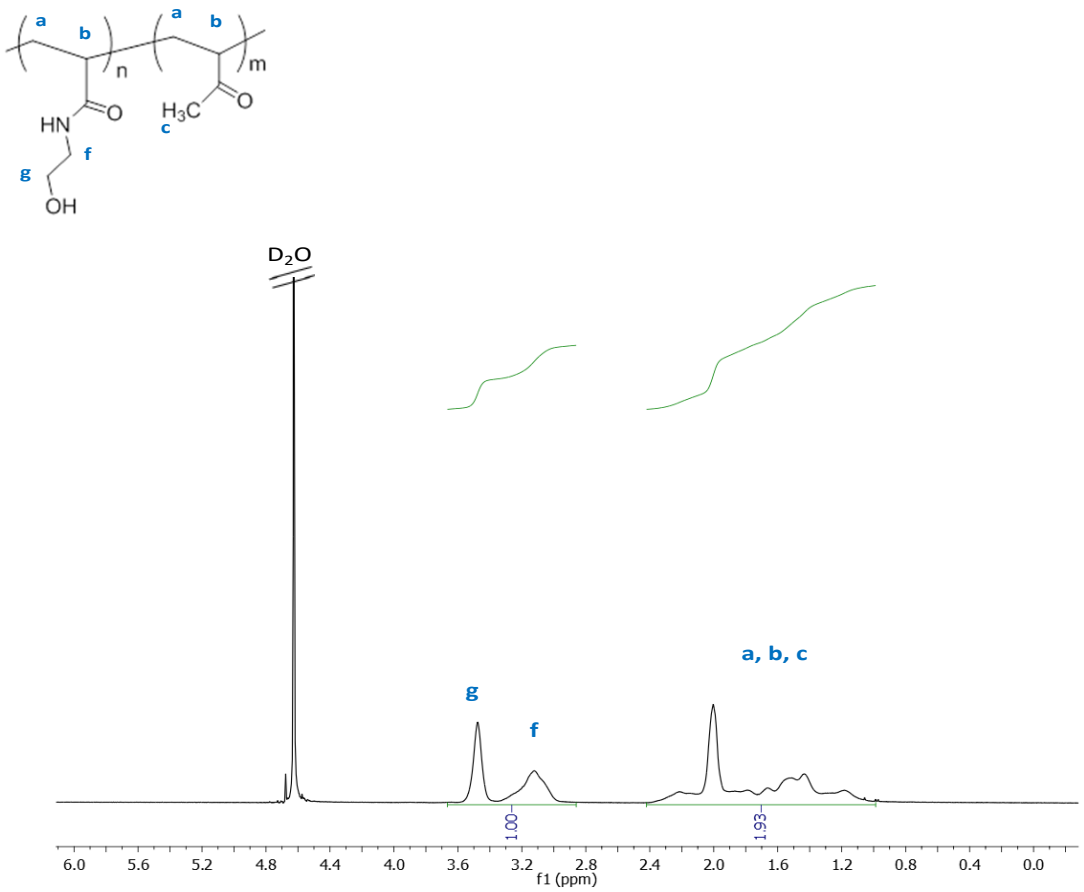

Figure S1. ^{1}H-NMR of PHEAA-*co*-PMVK (400 MHz, D_2O).

Chemical shifts: δ 3.12 ppm (-N-C**H**$_2$-C-), 3.47 ppm (-C-C**H**$_2$-O-), 2.01 ppm (-C**H**$_3$), 0.98-2.37 ppm (-C-C**H**$_2$-C**H**-C- [backbone protons]).

Copolymer composition was established by integration of peaks f and g (4n, I=1.0) and peaks a, b, c (6m+3n, I=1.93): n=0.25, m=0.19

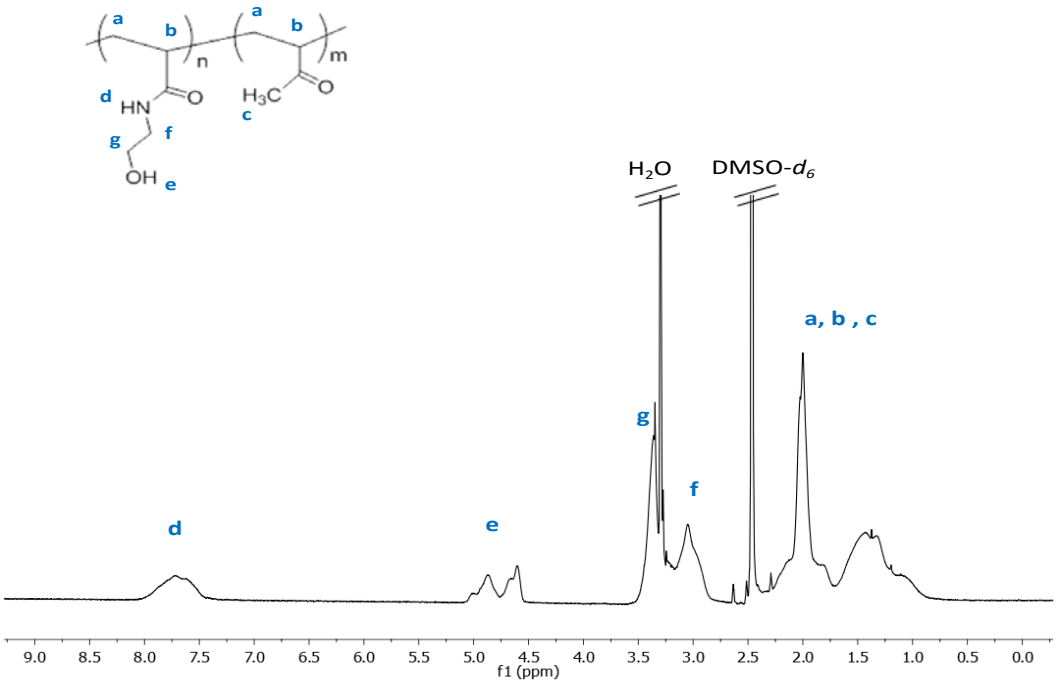

Figure S2. ^{1}H-NMR of PHEAA-*co*-PMVK (400 MHz, DMSO-d_6).

Chemical shifts: δ 7.70 ppm (-C-N**H**-C-), 4.53-5.09 ppm (-C-O**H**), 3.05 ppm (-N-C**H₂**-C-), 3.36 ppm (-C-C**H₂**-O-), 2.0 ppm (-C**H₃**), 0.86-2.26 ppm (-C-C**H₂**-C**H**-C- [backbone protons]).

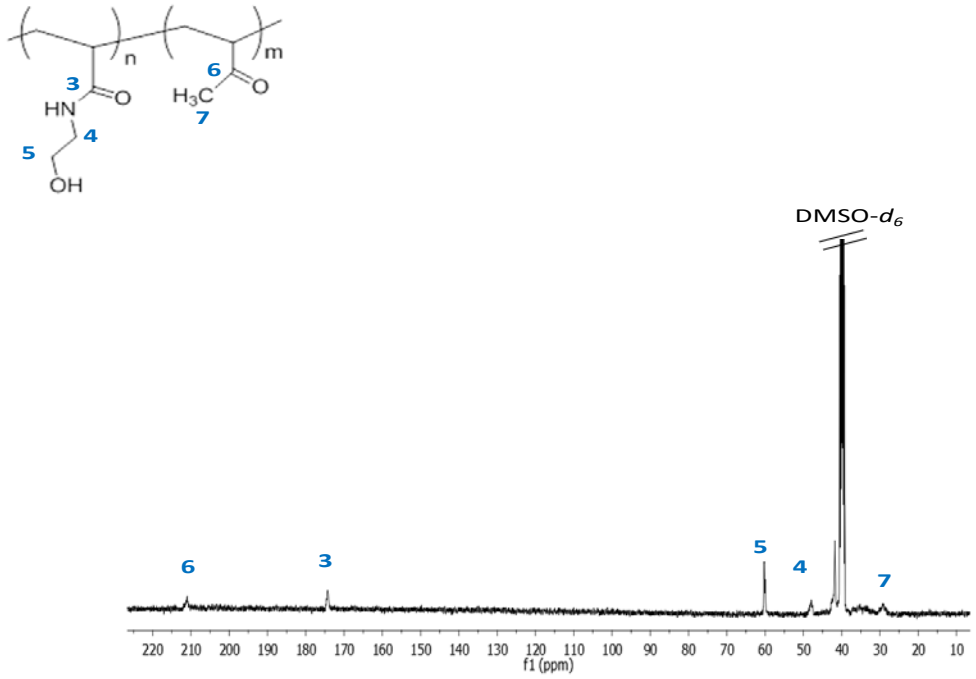

Figure S3. ^{13}C-NMR of PHEAA-*co*-PMVK (400 MHz, DMSO-d_6).

Chemical shifts: δ 29.04 ppm (-O=C-**C**H$_3$), 47.98 ppm (-NH-**C**H$_2$-C-), 59.80 ppm (-C-**C**H$_2$-OH), 174.20 ppm (-N-**C**=O), 211.03 ppm (C-**C**=O).

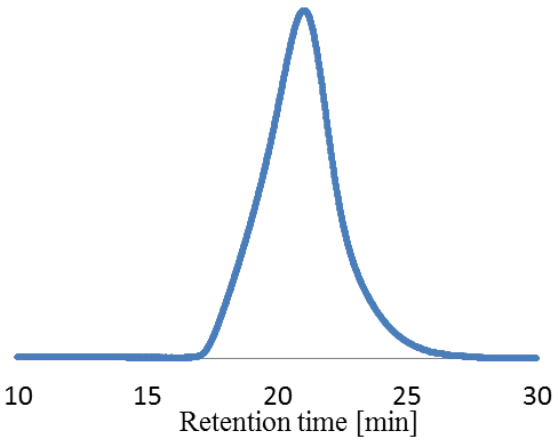

Figure S4. SEC traces of PHEAA-*co*-PMVK (M_n=284 kDa, $Đ$=2.39).

Synthesis of tetraethylene glycol bishydroxylamine (TEG-BHA):[1]

To a solution of tetraethylene glycol (2.0 g, 10.3 mmol), triphenylphosphine (8.1 g, 27.7 mmol) and N-hydroxyphthalimide (3.53 g, 21.6 mmol) in THF (160 mL) was added DIAD (6.25 mL, 31.7 mmol) in THF (40 mL) dropwise. The reaction was stirred at room temperature overnight before being concentrated under vacuum. The crude product was redissolved in a 80% ethyl acetate: 20% hexane solution causing crystallisation of the triphenylphosphine oxide (PPh3O) by-product which was removed via filtration. The filtrate was then concentrated under vacuum and purified by flash chromatography using ethyl acetate:hexane (50:50 increasing to 90:10). The product (N-hydroxyphthalimide protected TEG) was collected as a white solid (3.21 g, 64%). ^{1}H-NMR (400 MHz, $CDCl_3$): δ 7.70-7.62 (m, 8 H, Ph-H), 4.22 (bt, 4H, -CH2), 3.71 (bt, 4H, -CH2), 3.47 (bt, 4H, -CH2), 3.37 (bt, 4H, -CH2).

To the N-hydroxyphthalimide protected TEG (2.0 g, 4.1 mmol) in MeOH (30 mL) was added hydrazine monohydrate (0.81 mL, 16.6 mmol) and the solution stirred at room temperature overnight. The crude solution was filtered to remove the solid precipitate and the filtrate collected and concentrated under vacuum. An excess of HCl was added and the solution dried under vacuum. The resulting solid was washed thoroughly with DCM yielding the pure product as a pale yellow salt (1.15g, 94%).

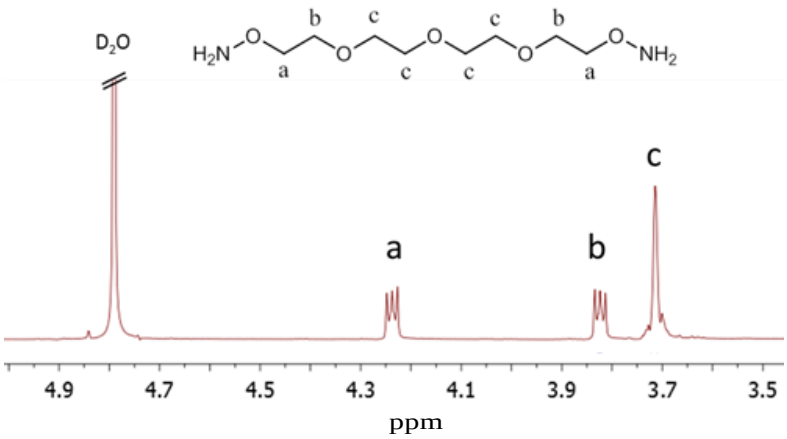

Figure S5. ^{1}H-NMR of TEG-BHA, (400 MHz, $CDCl_3$). Chemical shifts: δ 4.24 ppm (t, 4H, -C**H**$_2$), 3.82 ppm (t, 4H, -C**H**$_2$), 3.71ppm (s, 8H, -C**H**$_2$).

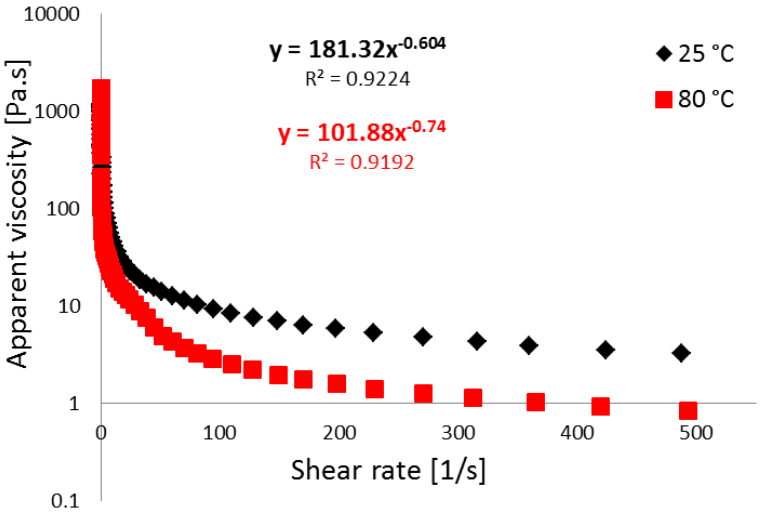

Figure S6. Flow curves of G_{oxime} at 25°C and 80°C. The gel shows a good fit to the power law model: $\eta\eta = KK\gamma\dot{\gamma}^{nn-1}$, where η is the apparent viscosity, K is the consistency index, $\dot{\gamma}\dot{\gamma}$ is the shear rate and n is the power law index. The gel exhibits a shear thinning behaviour

(n<1), making it suitable for 3DP.

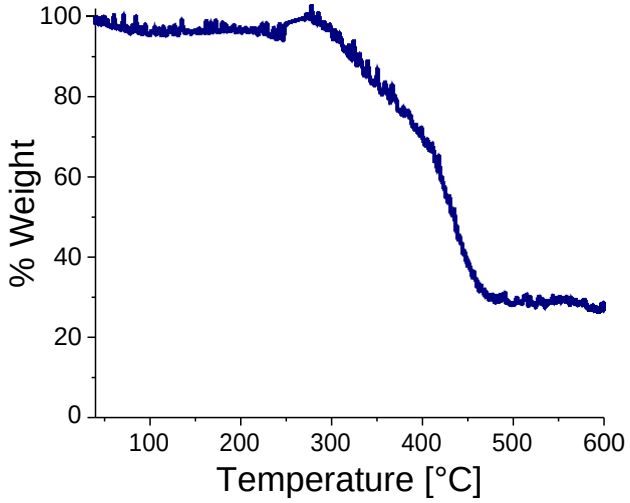

Figure S7. TGA curve of PHEAA-*co*-PMVK. The polymer exhibits high thermal stability (up to ~273°C), and no degradation signs were observed at 80°C (~96% of the original weight was retained, indicating stability).

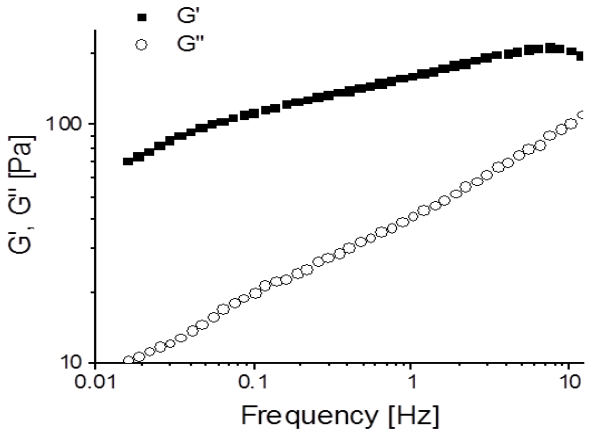

Figure S8. Frequency sweep of G_{oxime}. The gel exhibits frequency dependant behaviour, which indicates the dynamic nature of the gel forming bonds.

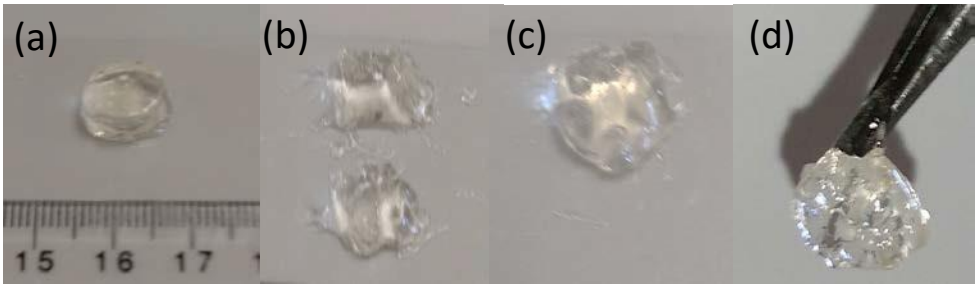

Figure S9. Self-healing of the 3D-printed G_{oxime}. (a) Intact 3D-printed G_{oxime} object. (b) The object after a scalpel cut. Due to the soft nature of G_{oxime} before TIPS treatment, the aggressive cut and the essential manual touching of the object resulted in its spreading and shape loss. (c) The pieces of the cut object were brought together to self-heal. (d) A self-healed object lifted as a single unit against gravity.

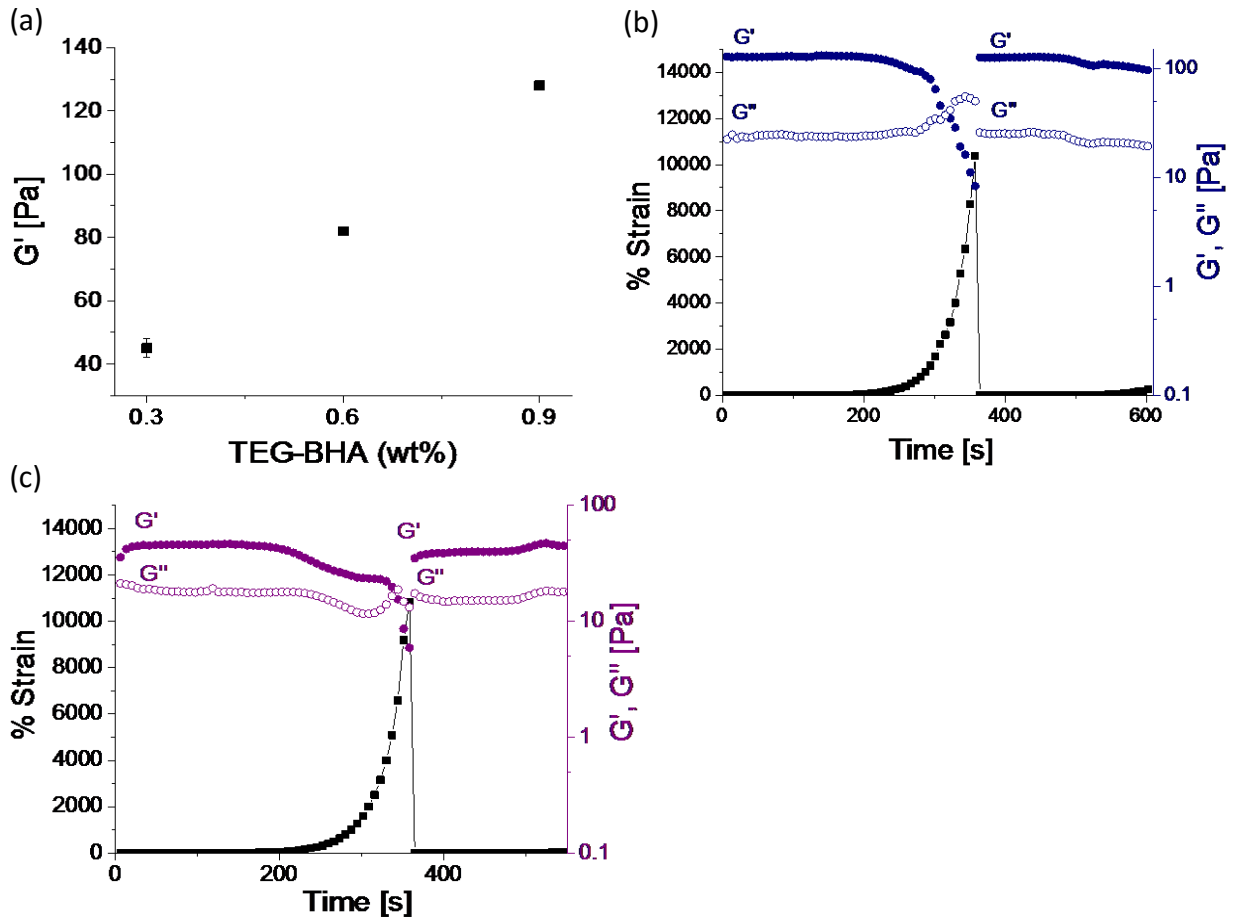

Figure S10. The effect of cross-linking on the mechanical and self-healing properties of oxime gels. Different wt% ratios of TEG-BHA to PHEAA-*co*-PMVK were examined: 0.3%, 0.6% (G_{oxime}), and 0.9%. (a) Storage modulus of the gels. The strength increases with the increasing degree of cross-linking. (b) Strain sweep of oxime gel with a high degree of cross-linking (0.9%wt TEG-BHA). The gel self-heals and fully recovers from high strains destruction. (c) Strain sweep of the soft oxime gel (0.3%wt TEG-BHA). The gel fully recovers from high strains damage and self-heals.

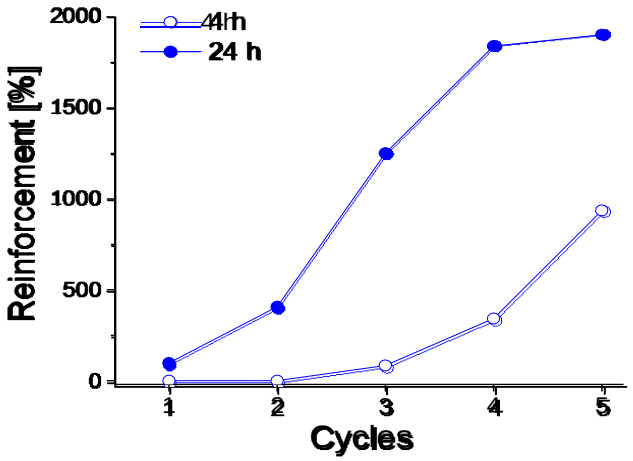

Figure S11. The effect of cryogelation time on the reinforcement of G_{oxime} (-10°C). When the freezing cycle was only 4 h, the reinforcement effect could not be achieved within the first 2 cycles. With the increasing number of cryogelation cycles, the reinforcement effect became more pronounced, until finally up to ~900% reinforcement was achieved. When the freezing cycles lasted 24 h, a gradual and significant reinforcement of up to ~1900% was achieved.

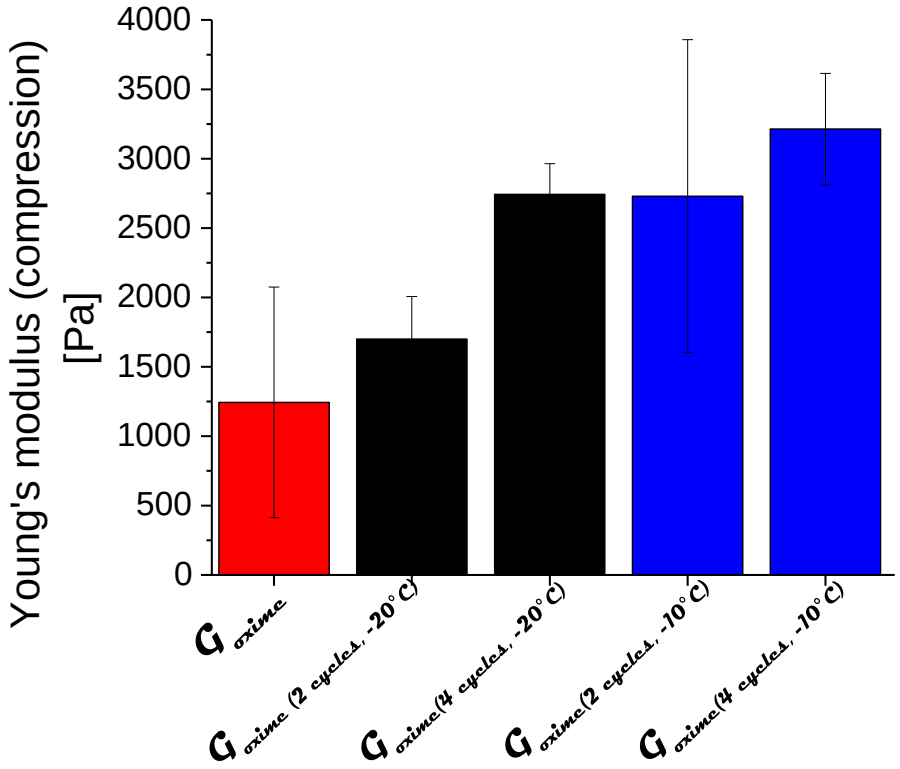

Figure S12. Young's (compression) modulus of G_{oxime} and the cryogels (average ±stdev are presented). Compression tests demonstrate a significant increase in Young's modulus with the increasing number of cryogelation cycles. In a good agreement with rheological characterization, the reinforcement effect is stronger at -10°C than at -20°C.

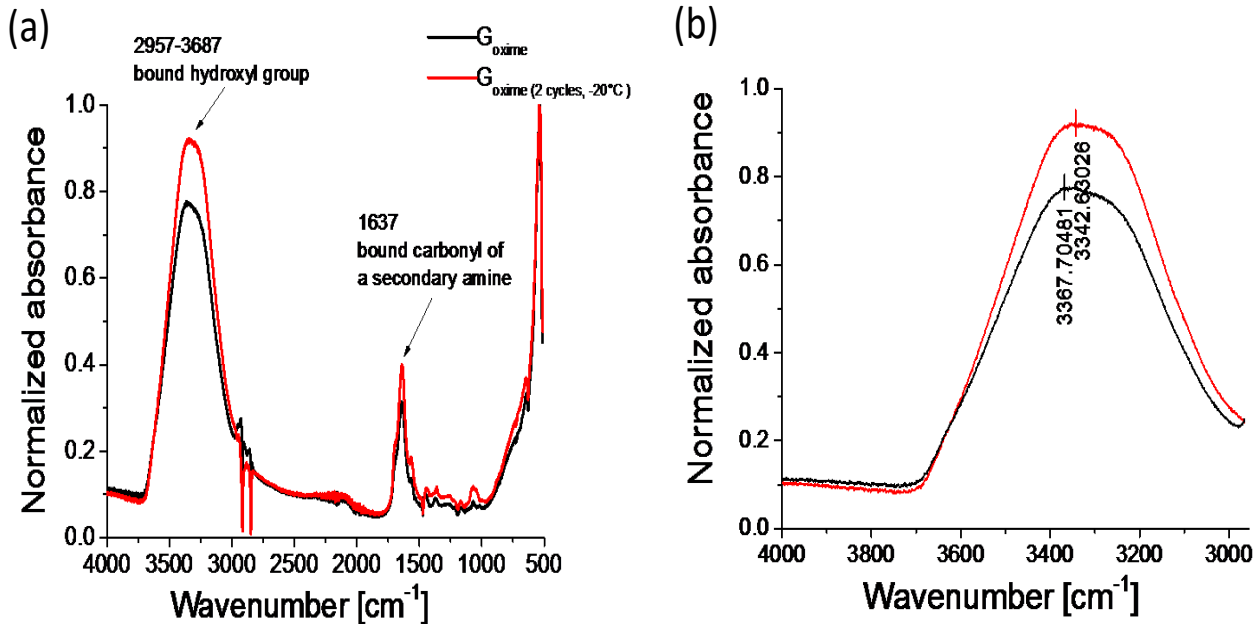

Figure S13. FTIR normalized spectra of G_{oxime} (black curve) and a representative oxime cryogel (2 freeze-thaw cycles,-20°C, red curve). (a) The spectra demonstrate the increase in hydrogen bonding after cryogelation, as evidenced by the increase in the intensity and the broadening of the bound hydroxyl groups peak (2957-3687 cm^{-1}), and the bound carbonyl stretching band of secondary amines (1637 cm^{-1}). (b) The bound hydroxyl peak shift from 3367 to 3342 cm^{-1} was also observed (indicated by the software peak analyser).

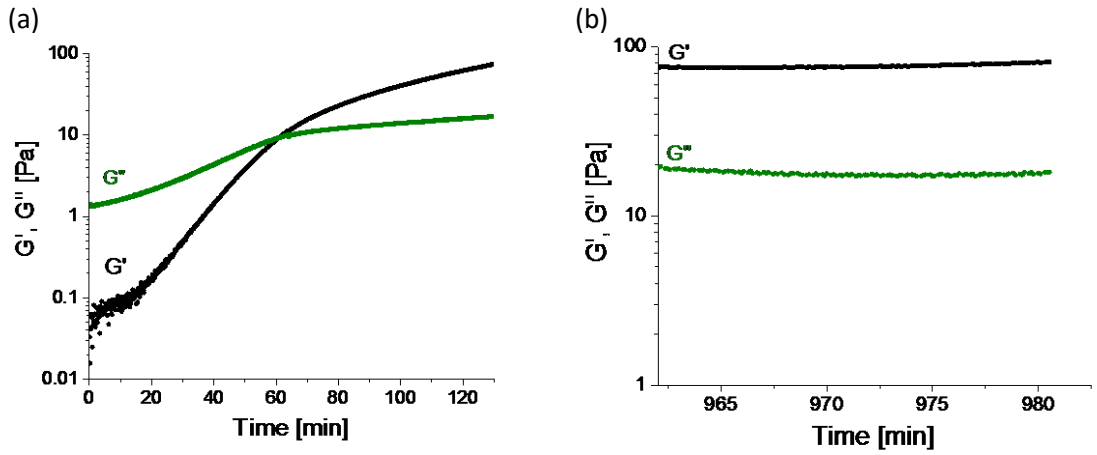

Figure S14. Gelation kinetics of G_{oxime}. (a) Sol-to-gel transition (crossover point) is observed after ~1 h of TEG-BHA introduction to PHEAA-*co*-PMVK solution. (b) Dynamic moduli of G_{oxime} 16 h after the cross-linking reaction was initiated. The moduli are fully stabilized overnight, indicating a complete maturation of the gel at ambient temperature.

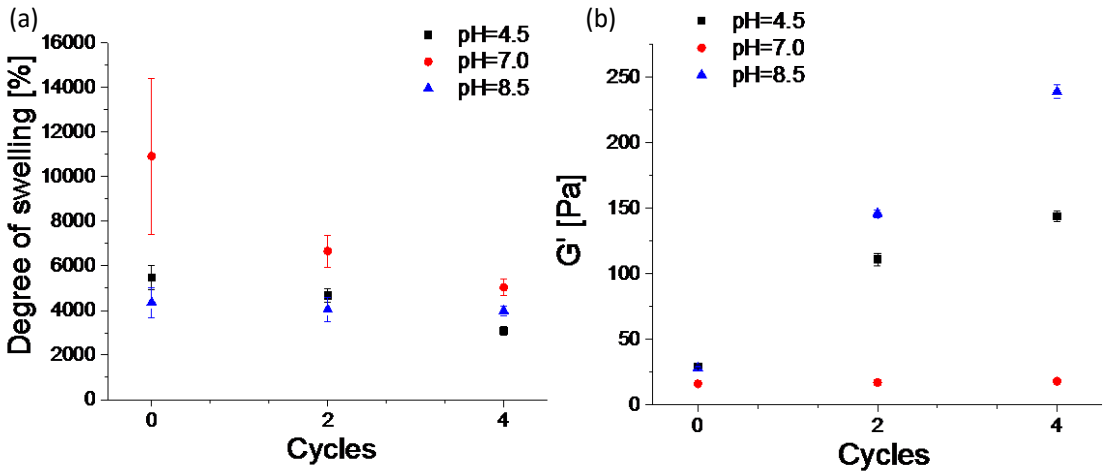

Figure S15. The effect of pH on G_{oxime} and the cryogels. (a) Degrees of swelling of G_{oxime} and the cryogels after 2 and 4 freeze-thaw cycles at -20°C at acidic, basic and neutral conditions. (b) Storage moduli of G_{oxime} and the cryogels after 2 and 4 freeze-thaw cycles at -20°C at acidic, basic and neutral conditions. The storage modulus values at pH=7.0 presented here are after gels swelling in deionized water (to be comparable with gels swollen in acid and base), and are therefore lower than the values reported in Figure 3 (gels as prepared).

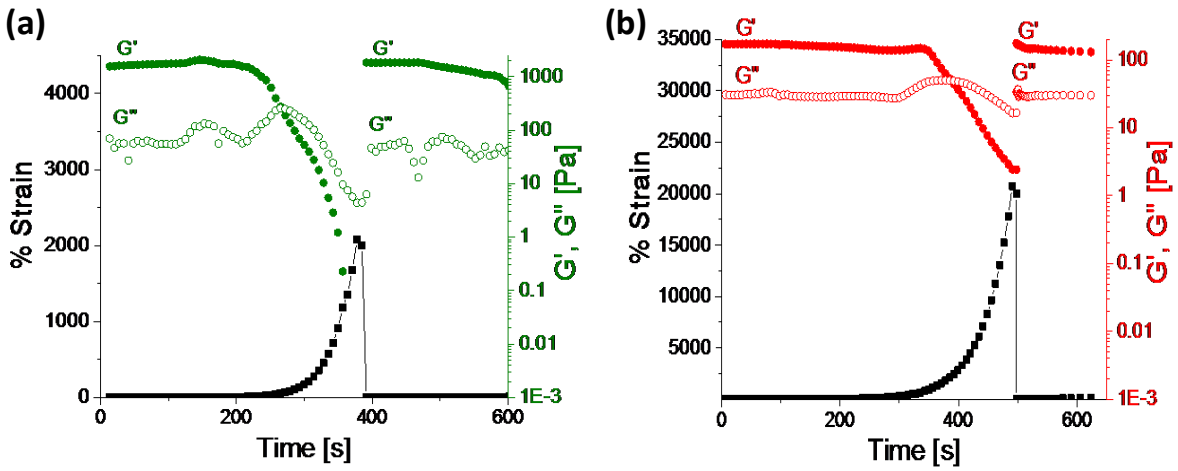

Figure S16. Self-healing of the cryogles characterized by rheology (curves of representative cryogels are demonstrated). (a) G_{oxime} after 4 freeze-thaw cycles at -10°C. The cryogel exhibits an immediate recovery from the network destruction. (b) G_{oxime} after 2 freeze-thaw cycles at -20°C. The cryogel instantly self-heals.

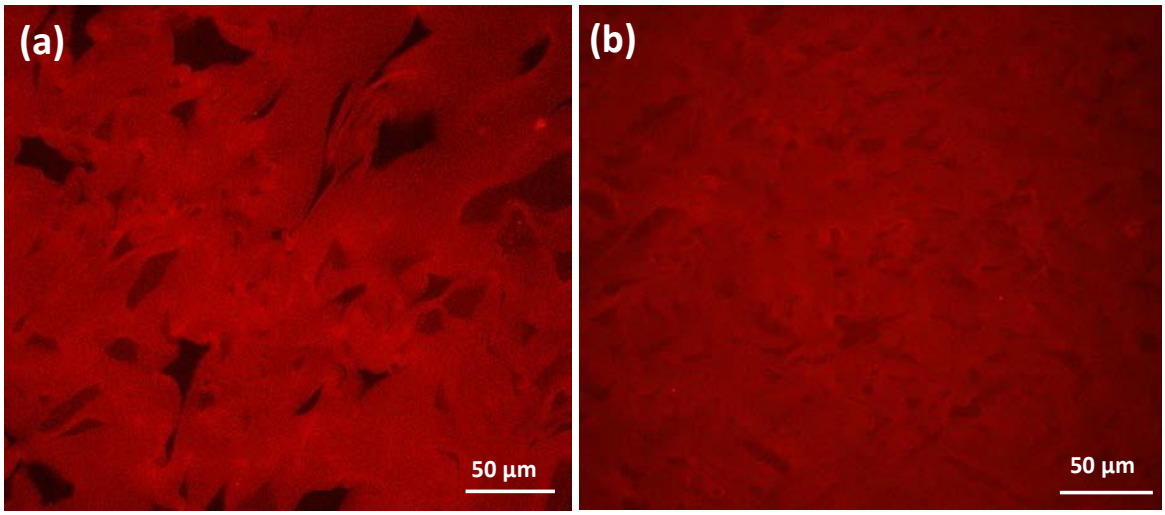

Figure S17. Morphological characterization of the cryogels prepared by subjecting G_{oxime} to 2 TIPS cycles. (a) Cryogel prepared at -10°C (average pore size of 23.5 µm and wall size of 7.4 µ). (b) Cryogel prepared at -20°C (average pore size of 6.4 µm and wall size of 4.0 µm).

References

[1] F. Taraballi, L. Russo, C. Battocchio, G. Polzonetti, F. Nicotra and L. Cipolla, *Org. Biomol. Chem.*, 2014, **12**, 4089–4092.